Supplemental Material

Figure S1. Reproducibility of ATAC in germ cells. (A) Scatterplot of ATAC-seq read counts from replicate B6 spermatocytes using 100,000 cells. (B) Distribution of insert size metrics for B6 ATAC-seq replicates from *A* showing clear nucleosome profile. (C) Enrichment of open chromatin around TSS sites from ATAC-seq replicates from *A*. (D) Scatterplot of ATAC-seq read counts from replicate KI spermatocytes using 100,000 cells. (E) Distribution of insert size metrics for KI ATAC-seq replicates from *D* and (B6xCAST)F1 showing clear nucleosome profile. (F) Similar to *C* showing TSS enrichment for KI and (B6xCAST)F1 samples. (G) Heat maps of H3K4me3, H3K9ac, and ATAC signals spanning ±1kb of previously identified PRDM9 motif locations. Heat maps are normalized reads per million (rpm) in 10 bp bins ordered by descending H3K4me3 level. Color scale is maintained across all panels. (H) Meta-profile of H3K4me3 level and open chromatin at recombination hotspots from KI spermatocytes anchored by $PRDM9^{Cst}$ motif (n = 9,305) scaled to maximum value to highlight positional relationship between nucleosome occupancy and open chromatin. (I) ATAC-seq cleavage footprint for $PRDM9^{Cst}$ show poor protection from Tn5 cutting across $PRDM9^{Cst}$ motif (n = 4,014 ATAC peaks that overlap $PRDM9^{Cst}$ motif) (J) Meta-profile of H3K4me3 (red) and ATAC (grey) signals at CTCF sites. CTCF ChIP-seq data is from modENCODE project (Shen et al., 2012). Only CTCF sites that did not overlap TSS were used (n = 2,926 ATAC peaks that overlap CTCF motif). Signals are background subtracted and scaled to maximum value. (K) Similar to *I* except for CTCF locations from *J* showing protection from cutting across CTCF motif locations (motif used in analysis shown above).

Figure S2. *Hells* is expressed in spermatagonia and leptotene stages. (A-F) t-SNE plots of single-cell RNA-seq from adult B6 testis (Jung et al., 2019) arranged by pseudo-time. All t-SNE plots were created using the testis Atlas shiny app (http://www.stats.ox.ac.uk/~wells/testisAtlas.html). (A) Highlighted cells are from cluster 5 annotated as leptotene stage. Arrow indicates pseudotime of spermatogenesis from spermatogonia to sperm. Individual meiotic stages are indicated by different colors. (B) t-SNE plot showing cells expressing *Prdm9* found largely in cluster 5 indicating leptotene stage. (C) t-SNE plot showing expression of *Hells* in spermatogonia and leptotene stages. (D) t-SNE plot showing *Ino80* expression across multiple stages of spermatogenesis.

Figure S3. Meiotic-specific loss of *Hells* leads to zygotene/early-pachytene block. (A) Immunolabeling of cross-sections from *Hells* CKO adult testis show loss of HELLS expression, persistence of DSBs in the most advanced meiotic cells, and lack of post-meiotic cells. Sections

were immunolabeled with anti-HELLS (red) and anti-γH2AFX (green). Nuclei were counterstained with DAPI in blue. Scale bar = 100 μm. (B) Chromatin spreads of spermatocytes from *Hells* control and CKO animals displaying representative images of meiotic substages scored to determine meiotic block in **Fig. 3F**. Spreads were immunolabeled with anti-γH2AX (red) as an indicator of double-strand breaks and anti-SYCP3 (red) to allow visualization chromosome condensation. Scale bar = 10 μm.

Figure S4. Loss of *Hells* results in decreased H3K4me3 at hotspots. (A) Upper – dendrogram of hierarchical clustering (Euclidean distance) showing relationship among H3K4me3 ChIP-seq libraries for different mouse strains. Lower – boxplot comparing distribution of H3K4me3 level at hotspots (blue) compared to all other loci (grey). B6 12 dpp H3K4me3 ChIP-seq samples are from (Baker et al., 2014). (B) Scatterplot comparing single *Hells* CKO sample to age-matched B6 sample. Hotspots (blue) show higher H3K4me3 level in B6 compared to *Hells* CKO, while all other H3K4me3 sites (black) are more similar. Linear regression lines are plotted separately for both classes of H3K4me3 sites. (C) Scatter plot similar to *B* comparing two *Hells* CKO replicates. (D) Linear regression of pair-wise comparison between B6, *Hells* wild-type, and *Hells* CKO H3K4me3 ChIP samples. Linear regression lines are plotted separately for hotspots (blue) and all other H3K4me3 sites (black). Plot from panel *B* is highlighted in yellow and plot from panel *C* is highlighted in red.

Figure S5. Testis from juvenile mice display similar stages of early meiotic progression in the absence of HELLS (A) 12 dpp testis cross-sections, stained with PAS, of *Hells* heterozygous control and CKO testis. (B) Western blot of whole cell protein extract from whole testis (2 testis per genotype) collected from *Hells* homozygous controls, *Hells* CKO, and *Prdm9*$^{-/-}$ (P9KO). Western blots for *Hells* genotypes were collected from age-matched littermates and show two additional replicate Western blots in addition to **Figs. 5A and 6G**. Blots were decorated with anti-HELLS and anti-PRDM9, anti-β-Tubulin serves as a loading control. (C) Quantification of Western blots comparing PRDM9 expression levels between *Hells* CKO and age-matched littermate controls. Within each replicate the levels of PRDM9 in heterozygous control animals is set to one (replicate 1 is from **Fig. 5A**, replicate 4 is from **Fig. 6G**). β-tubulin was used as a loading control. (D) Immunolabeling of 12 dpp testis cross-sections of *Hells* heterozygous control and CKO testis show loss of HELLS expression in meiotic cells from CKO mice (arrow head – HELLS expression in pre-meiotic cells prior to Stra8-iCre expression, asterisk – incomplete loss of HELLS likely due to leaky *Cre* expression). In the absence of HELLS, PRDM9 expression is still detected along with DSBs. Sections were immunolabeled

with anti-HELLS (red), anti-PRDM9 (magenta), and anti-P-H2AFX (green). Nuclei were counterstained with DAPI in blue. Scale bars = 50 µm

Figure S6. HELLS binds at promoters. (A) Profile of ATAC-seq, H3K4me3 ChIP-seq, IgG control, and HELLS ChIP-seq, at the *Sycp1* promoter in germ cells collected from PRDM9^{Cst} hotspot in KI mice. RNA-seq expression profile is from B6 germ cells. (B) Boxplot comparing distribution of gene expression (log2 transcripts per million, tpm) with (grey, n = 606) or without (black, n = 14,419) a HELLS ChIP-seq peak at their respective promoters (mean ± SEM, *p* value – Welch's two-sided test). (C) Meta-profile of H3K4me3 (red) and HELLS (grey) signals at gencode TSS that overlap HELLS ChIP-seq peaks (n = 633). Signals are background-subtracted and scaled to maximum value to highlight positional relationship between nucleosome position and HELLS binding.

Table S1. High throughput sequencing libraries used in this study.

Table S2. **Oligonucleotides used for quantitative PCR in this study.**

Figure S1

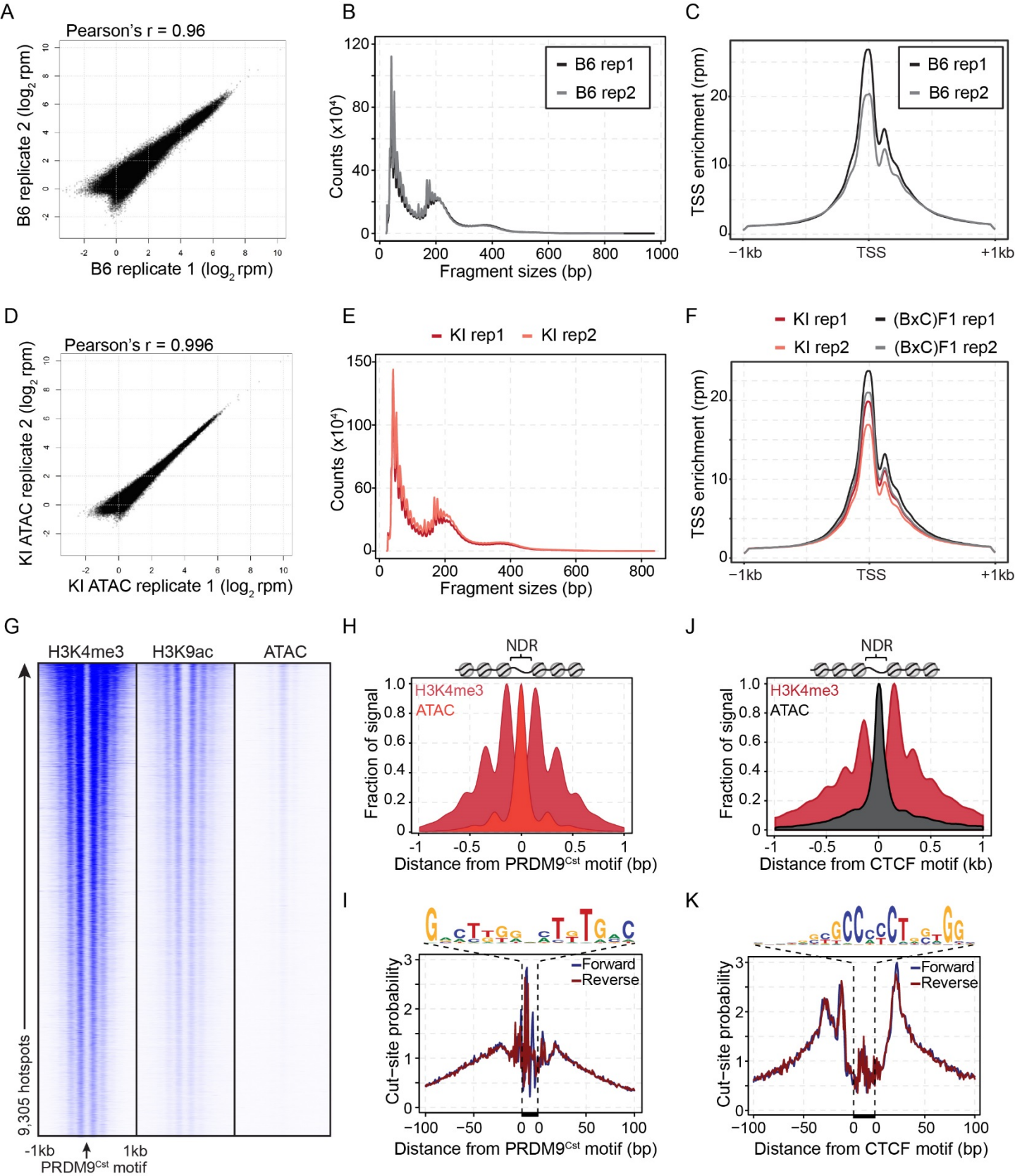
A
Pearson's r = 0.96
B6 replicate 2 (log2 rpm)
B6 replicate 1 (log2 rpm)
B
B6 rep1
B6 rep2
Counts (x10⁴)
Fragment sizes (bp)
C
B6 rep1
B6 rep2
TSS enrichment (rpm)
−1kb
TSS
+1kb
D
Pearson's r = 0.996
KI ATAC replicate 2 (log2 rpm)
KI ATAC replicate 1 (log2 rpm)
E
KI rep1
KI rep2
Counts (x10⁴)
Fragment sizes (bp)
F
KI rep1
KI rep2
(BxC)F1 rep1
(BxC)F1 rep2
TSS enrichment (rpm)
−1kb
TSS
+1kb
G
H3K4me3
H3K9ac
ATAC
9,305 hotspots
-1kb
1kb
PRDM9Cst motif
H
NDR
H3K4me3
ATAC
Fraction of signal
Distance from PRDM9Cst motif (bp)
J
NDR
H3K4me3
ATAC
Fraction of signal
Distance from CTCF motif (kb)
I
Forward
Reverse
Cut-site probability
Distance from PRDM9Cst motif (bp)
K
Forward
Reverse
Cut-site probability
Distance from CTCF motif (bp)

Figure S2

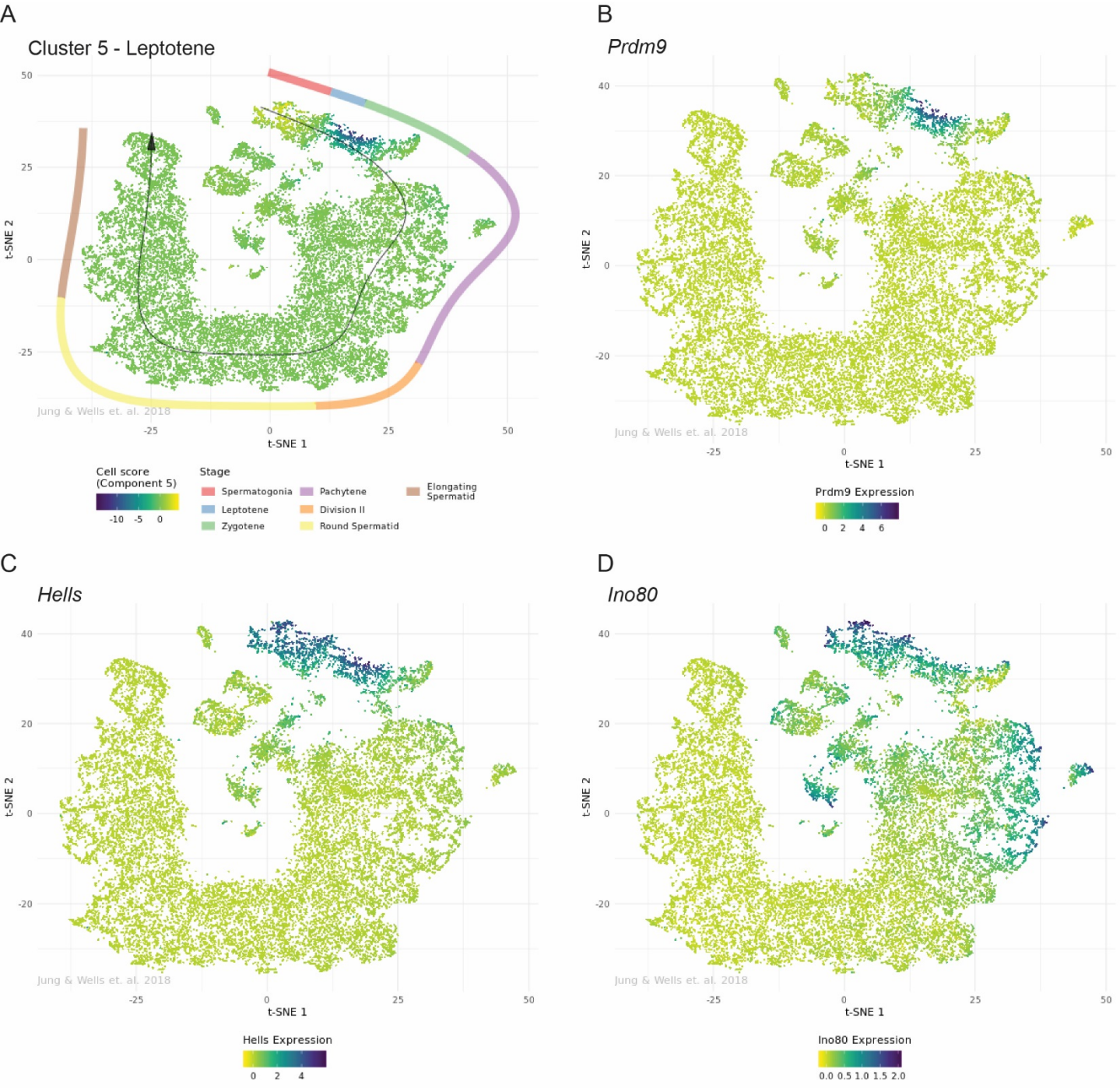
A
Cluster 5 - Leptotene
t-SNE 2
t-SNE 1
Jung & Wells et. al. 2018
Cell score (Component 5)
-10 -5 0
Stage
Spermatogonia
Leptotene
Zygotene
Pachytene
Division II
Round Spermatid
Elongating Spermatid
B
Prdm9
Prdm9 Expression
0 2 4 6
C
Hells
Hells Expression
0 2 4
D
Ino80
Ino80 Expression
0.0 0.5 1.0 1.5 2.0

Figure S3

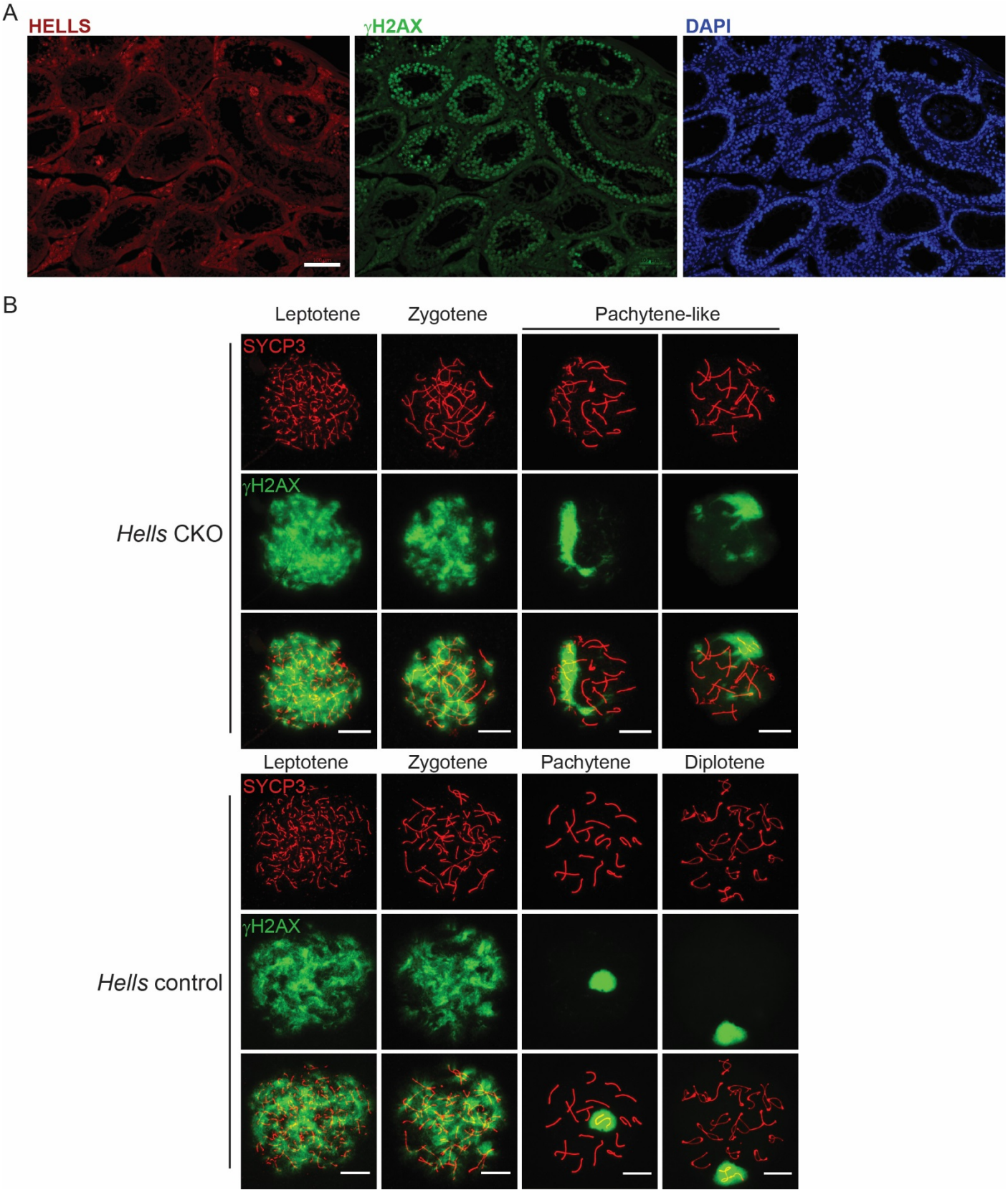
A
HELLS
γH2AX
DAPI
B
Leptotene
Zygotene
Pachytene-like
SYCP3
γH2AX
Hells CKO
Leptotene
Zygotene
Pachytene
Diplotene
SYCP3
γH2AX
Hells control

Figure S4

A

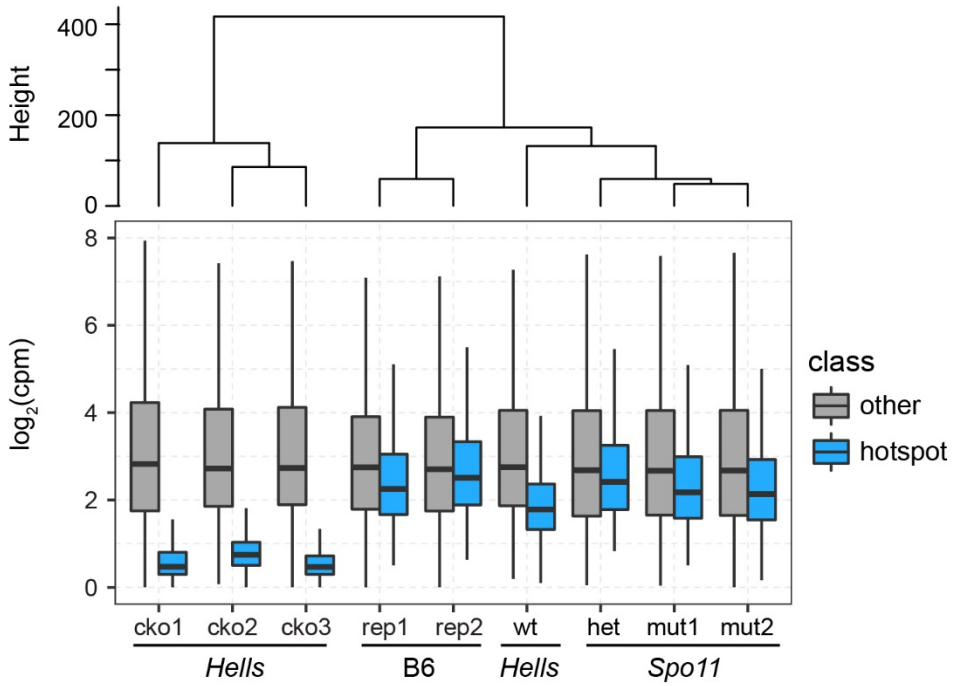

B

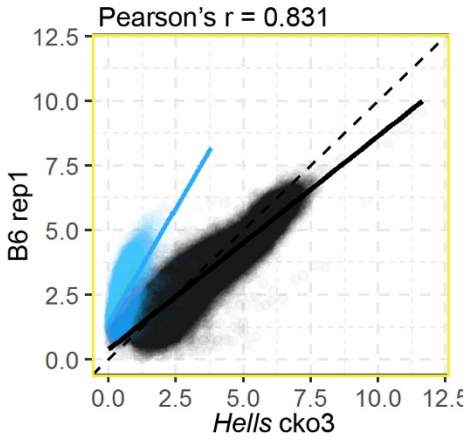

C

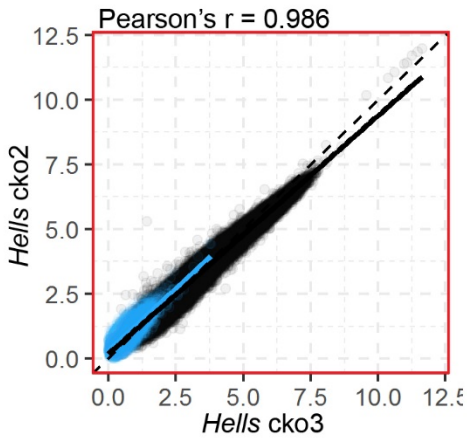

D

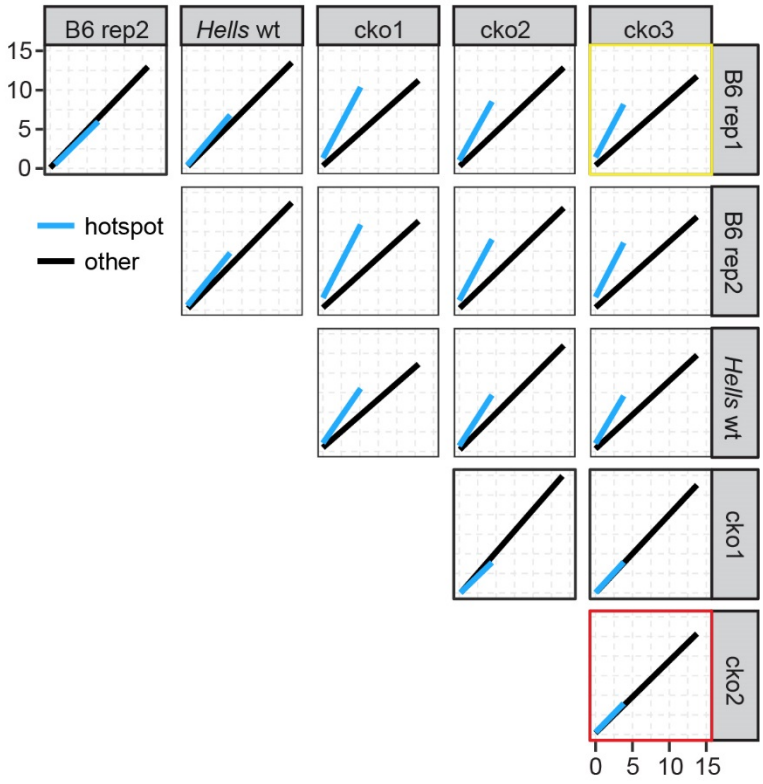

Figure S5

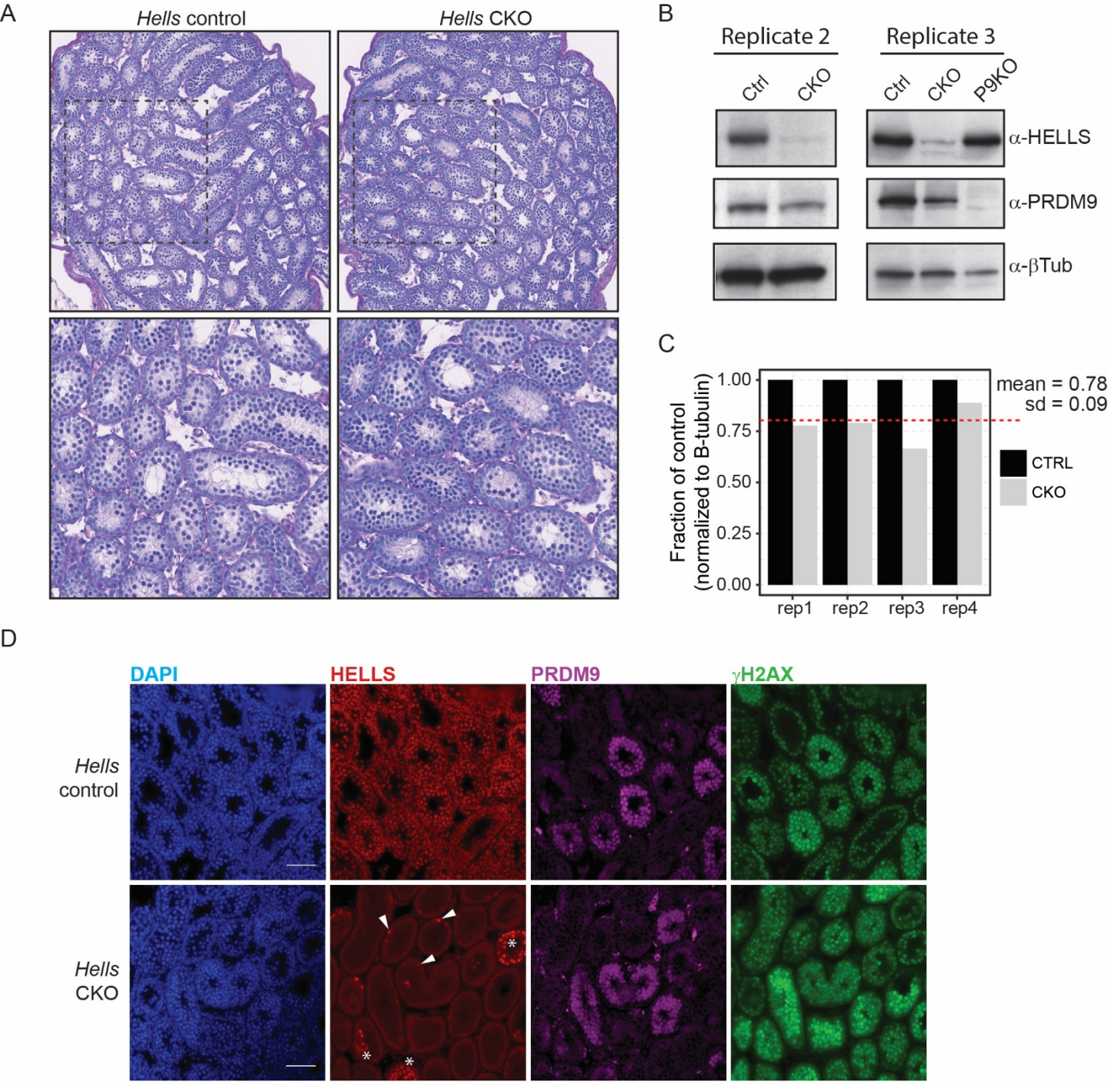
A
Hells control
Hells CKO
B
Replicate 2
Replicate 3
Ctrl
CKO
Ctrl
CKO
P9KO
α-HELLS
α-PRDM9
α-βTub
C
Fraction of control
(normalized to B-tubulin)
1.00
0.75
0.50
0.25
0.00
mean = 0.78
sd = 0.09
CTRL
CKO
rep1
rep2
rep3
rep4
D
DAPI
HELLS
PRDM9
γH2AX
Hells
control
Hells
CKO

Figure S6

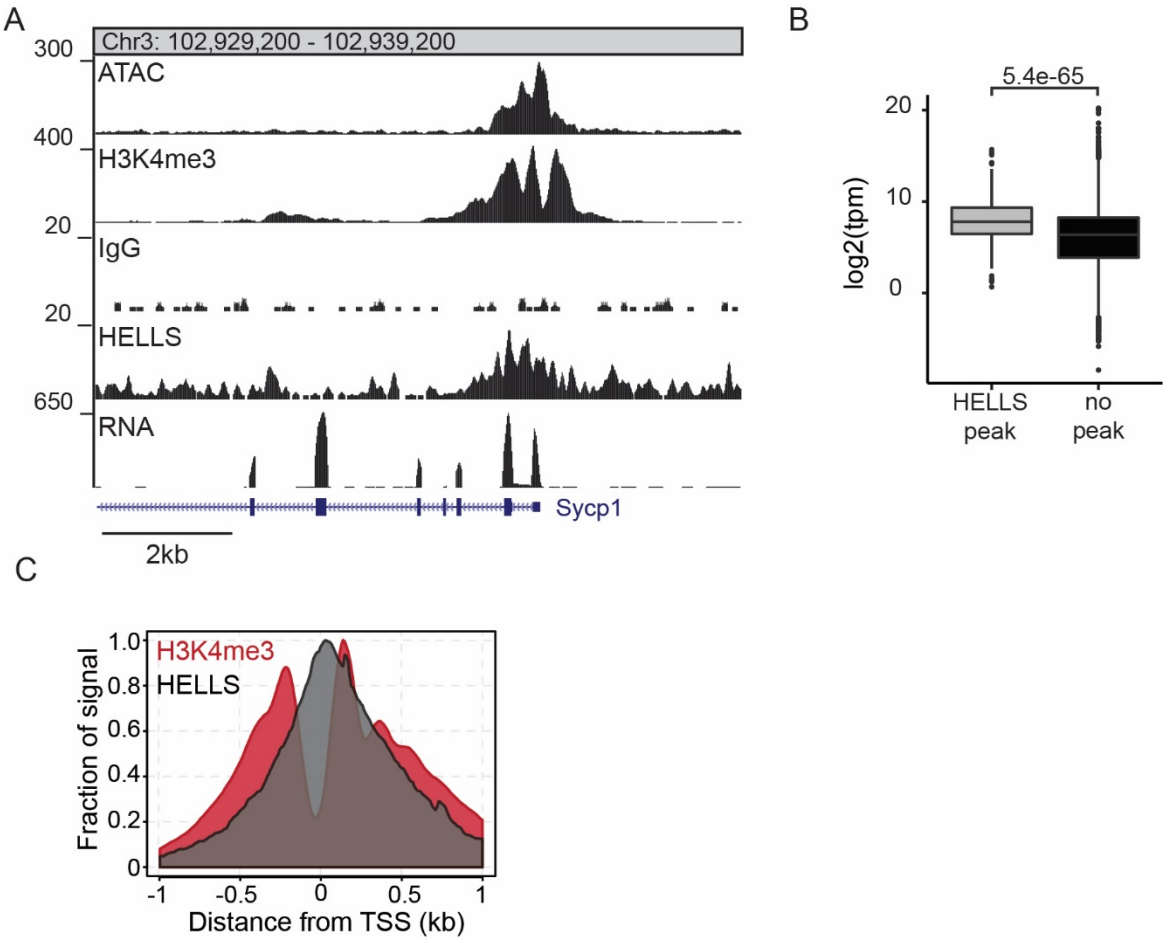
A
Chr3: 102,929,200 - 102,939,200
300
ATAC
400
H3K4me3
20
IgG
20
HELLS
650
RNA
Sycp1
2kb
B
5.4e-65
20
10
0
log2(tpm)
HELLS peak
no peak
C
H3K4me3
HELLS
Fraction of signal
1.0
0.8
0.6
0.4
0.2
0
-1
-0.5
0
0.5
1
Distance from TSS (kb)

name	strain	antibody	age	GEO
ATAC4	C57BL/6J	atac	14 dpp	GSE135896
ATAC7	C57BL/6J	atac	14 dpp	GSE135896
ATAC13	CAST_KI	atac	14 dpp	GSE135896
ATAC14	CAST_KI	atac	14 dpp	GSE135896
ATAC15	DBA/2J	atac	14 dpp	GSE135896
ATAC16	DBA/2J	atac	14 dpp	GSE135896
ATAC17	(B6xCAST) F1	atac	14 dpp	GSE135896
ATAC18	(B6xCAST) F1	atac	14 dpp	GSE135896
ATAC56	Spo11/+	atac	14 dpp	GSE135896
ATAC57	Spo11 mutant	atac	14 dpp	GSE135896
ATAC58	Spo11 mutant	atac	14 dpp	GSE135896
ATAC61	Hells mutant	atac	12 dpp	GSE135896
ATAC62	Hells wt	atac	12 dpp	GSE135896
ATAC84	Hells mutant	atac	12 dpp	GSE135896
ATAC85	Hells wt	atac	12 dpp	GSE135896
ATAC86	Hells mutant	atac	12 dpp	GSE135896
chip1	Spo11 mutant	H3K4me3	14 dpp	GSE135896
chip2	Spo11 control	H3K4me3	14 dpp	GSE135896
chip9	Hells mutant	input	12 dpp	GSE135896
chip10	Spo11 mutant	H3K4me3	14 dpp	GSE135896
chip11	Spo11 mutant	H3K9ac	14 dpp	GSE135896
chip15	Hells mutant	H3K4me3	12 dpp	GSE135896
chip16	Hells wt	DMC1	6 weeks	GSE135896
chip17	Hells wt	DMC1	6 weeks	GSE135896
chip18	Hells wt	input	6 weeks	GSE135896
chip19	Hells mutant	DMC1	6 weeks	GSE135896
chip20	Hells mutant	DMC1	6 weeks	GSE135896
chip21	Hells mutant	input	6 weeks	GSE135896
chip22	Hells mutant	H3K4me3	12 dpp	GSE135896
chip23	Hells wt	H3K4me3	12 dpp	GSE135896
chip34	CAST_KI	HELLS	12 dpp	GSE135896
chip35	CAST_KI	IgG	12 dpp	GSE135896
chip37	CAST_KI	HELLS	12 dpp	GSE135896
chip39	CAST_KI	input	12 dpp	GSE135896
chip40	Hells mutant	H3K4me3	12 dpp	GSE135896
AL2	C57BL/6J	H3K4me1	12 dpp	GSE135896
AM2	C57BL/6J	H3K9me2	12 dpp	GSE61613
AN2	C57BL/6J	H3K4me1	12 dpp	GSE135896
AO	C57BL/6J	H3K9me2	12 dpp	GSE61613
AX2	C57BL/6J	H3K27me3	14 dpp	GSE135896
BR	(B6xCAST) F1	H3K9ac	12 dpp	GSE135896
BV2	C57BL/6J_NaBut	H3K9ac	14 dpp	GSE135896
BW2	C57BL/6J_NaBut	H3K27ac	14 dpp	GSE135896
BY	C57BL/6J_NaBut	H2B120ac	14 dpp	GSE135896
CB2	C57BL/6J	H3K27me3	14 dpp	GSE135896
CF	C57BL/6J	H2A.Z	14 dpp	GSE135896

CG2	C57BL/6J	H3K9ac	14 dpp	GSE135896
CH2	C57BL/6J_NaBut	H3K9ac	14 dpp	GSE135896
CI2	C57BL/6J_NaBut	H3K27ac	14 dpp	GSE135896
CJ	CAST_KI	H3K9ac	14 dpp	GSE135896
CK	CAST_KI	H3K9ac	14 dpp	GSE135896
hui1	C57BL/6J	H3K9me3	14 dpp	GSE61613
natalie1	C57BL/6J	H3K36me3	14 dpp	GSE76416
germ_B6-rep3	C57BL/6J	H3K4me3	14 dpp	GSE113192
germ_D2-rep1	DBA/2J	H3K4me3	14 dpp	GSE113192
B6xKI_H3K4me3_ChIP_sample_1	(B6xCAST) F1	H3K4me3	12 dpp	GSE52628
B6xKI_H3K4me3_ChIP_sample_2	(B6xCAST) F1	H3K4me3	12 dpp	GSE52628
KI_H3K4me3_ChIP_sample_1	CAST_KI	H3K4me3	12 dpp	GSE52628
KI_H3K4me3_ChIP_sample_2	CAST_KI	H3K4me3	12 dpp	GSE52628

Purpose	Name	Sequence
Hells genotyping	Hells_1	GTAAGAGTCTCAGTGTCAACC
	Hells_2	CAACGGGTTCTTCTGTTAGTCC
	Hells_3	AAGTCGTCGTCCTTACCAGTG
	Hells_4	AGGACTCCAGGCAAATCTGA
ChIP-qPCR	C1_114_peak_1F	CTGCCTTCATTCCACTCCTC
	C1_114_peak_1R	CAGGGAGGGAAAACATAAATCA
	C1_114_valley_2F	TGTTCCACACCCAGCTATTG
	C1_114_valley_2R	ATCATGGGGCAAGATCAAAC
	C2_44_peak_1F	CTTGTAGAACTGAGATTAGTTGAGAGC
	C2_44_peak_1R	GCTTTTCCTGTTTCTCCCCTA
	C2_44_valley_2F	CACTGGGGATGGTAGCATTAG
	C2_44_valley_2R	TCAAGGACACAGGGGATGAT
	C3_F	ATTGCTAGAAAGGCGTGTGC
	C3_R	TTGCTAGGCATGTGAAATGG
	A1_1F	AACTGCACAGCTGCAAACAC
	A1_1R	TATCCCAACCAATCCCATGT
	hGAPDH_F	GAGCCTCGAGGAGAAGTTCC
	hGAPDH_R	GACTGAGATGGGGAATTGGA

notes

to genotype tm1a use Hells_1 and Hells_2; expected size 663bp

to genotype tm1c use Hells_3 and Hells_4; wt expected size 323 bp mutar
to genotype tm1d use Hells_1 and Hells_4; expected mut size 705 bp
Figure 6B, 6C
Figure 6B, 6C
Figure 6C, 6H, 7A
Figure 6C, 6H, 7A
Figure 6B, 6C
Figure 6B, 6C
Figure 6C, 6H, 7A
Figure 6C, 6H, 7A
Figure 6H, 7A
Figure 6H, 7A
Figure 6C, 6H, 7A
Figure 6C, 6H, 7A
Figure 6C, 6H, 7A
Figure 6C, 6H, 7A

ıt size 385 bp